Acta Cryst. (1973). B29, 1604

Uses of a Native Anomalous Scatterer in a Protein Structure Determination

BY PATRICK ARGOS* AND F. SCOTT MATHEWS

Washington University School of Medicine, Departments of Physiology and Biophysics and of Biological Chemistry, 660 South Euclid, St. Louis, Missouri 63110, U.S.A.

(*Received* 4 *October* 1972; *accepted* 12 *March* 1973)

A detailed discussion of the uses of the iron atom as an anomalous scatterer in the structure determination of the heme-containing protein, calf liver cytochrome b_5, is given. Anomalous scattering measurements at 2·8 Å resolution from native and derivative crystals were used to find (1) the location of the iron atom, (2) the relative locations of the iron and heavy-atom binding sites, and (3) the absolute configuration of the protein molecule. X-ray phases based on the anomalous scattering data from the native crystal alone were used to calculate difference Fourier maps which indicated clearly the major heavy-atom binding sites, their relative locations, and the absolute configuration of the protein.

Introduction

The isomorphous replacement method has been used in protein crystallography for the last 15 years and accounts for the many successful protein structure determinations. More recently inclusion of anomalous scattering effects produced by the added heavy atoms has made the method much more powerful (North, 1965; Matthews, 1966). Relatively little use of anomalous scattering centers naturally present in protein molecules has, however, been made. The most notable example so far is in the High Potential Iron Protein of *Chromatium* in which the approximate location of the iron cluster was located from the Bijvoet-difference Patterson synthesis (Kraut, Strahs & Freer, 1968) and the absolute configuration of the protein was obtained from the Bijvoet-difference Fourier synthesis based on heavy atom phases (Strahs & Kraut, 1968).

In the structure determination of cytochrome b_5 (Mathews, Levine & Argos, 1972) extensive use was made of the anomalous scattering effect caused by the heme iron naturally present. The first part of this communication describes in more detail some of the novel uses made of the iron in that study. The second part presents a method, first suggested by Matthews (1969), of determining heavy atom positions, their relative locations and absolute configuration, based on anomalous scattering from the native protein.

Structure determination of cytochrome b_5

(*a*) *Crystallographic data*

A detailed discussion of the cytochrome b_5 structure investigation is given by Mathews, Levine & Argos (1972). A brief summary is given here to indicate the quality of data used to obtain the results discussed herein.

Crystals of calf-liver cytochrome b_5 are orthorhombic, space group $P2_12_12_1$ with unit-cell dimensions $a=64{\cdot}54$, $b=46{\cdot}04$, and $c=29{\cdot}91$ Å and contain 4 molecules per unit cell. X-ray data were collected on a Picker FACS-1 automated diffractometer (controlled by a PDP-8S computer) employing unfiltered Cu $K\alpha$ radiation, focal spot size $0{\cdot}4\times8{\cdot}0$ mm, at a take-off angle of 6°. A modification of the Wyckoff step-scan procedure (Wyckoff *et al.*, 1967) was employed with an ω scan of 0·30°, centered on the peak. Counts were accumulated at 0·01° intervals; the observed intensities were taken to be the largest sum of 18 consecutive intervals, which was a typical peak width at half height.

The native protein data to a resolution of 2·8 Å (4500 reflections) were measured twice for each reflection and merged. Friedel equivalent pairs of reflections were measured close together in time and were symmetrically disposed in reciprocal space about a mirror plane perpendicular to the φ-axis. The X-ray intensities were corrected for absorption, background, radiation damage, and Lorentz and polarization effects. The decay of the diffracted intensity was only about 5% in 60 hours; thus, a complete quadrant of 2·8 Å data was collected from a single crystal.

(*b*) *Location of the iron and heavy atoms*

The position of the single heme iron atom, which has an imaginary scattering factor component of 3·4 e for Cu $K\alpha$ radiation (*International Tables for X-ray Crystallography*, 1962), was determined from the 3-dimensional anomalous scattering difference Patterson synthesis. The iron atom was located at $x/a=0{\cdot}517$, $y/b=0{\cdot}060$, and $z/c=0{\cdot}647$. The peaks on the 3 Harker sections arising from the inter-iron vectors have densities about 4 times the background level. The map is shown in Mathews, Levine & Argos (1972).

The heavy-atom binding sites for two derivatives, mersalyl and uranyl acetate, were found by typical difference Patterson and superposition techniques. The positions of the two major sites for the mersalyl and the two major and four secondary sites for the UO_2^{2+}

* Present address: Department of Physics, Pomona College, Claremont, California 91711, U.S.A.

are given by Mathews, Levine & Argos (1972). The relative mean changes in structure factor due to isomorphous substitution ($\langle \Delta F_{iso} \rangle / \langle F_{nat} \rangle$) were 39% for UO_2^{2+} and 17% for mersalyl. The relative mean differences due to anomalous scattering ($\langle |F(+) - F(-)| \rangle / \langle F \rangle$) were 9·4% for UO_2^{2+}, 4·7% for mersalyl, and 3·3% for the native data.

(c) *Determination of common origin*

Although the iron, mercury and uranyl sites were self consistent within each set, the origin of each set could be chosen arbitrarily at the origin, edge, face or body center of the unit cell. The derivative anomalous scattering difference Patterson maps were used to locate the origin and configuration of the heavy-atom sites relative to the iron atoms of the protein molecule. Each map will contain 4 cross vectors between the iron atom and each heavy atom site. Table 1 lists the Patterson density, summed over the 4 expected vectors for each major heavy-atom site for the 16 possible combinations of relative origin and configuration. The cumulative sum for each derivative is also given, since the relative positions of the major sites within each derivative were known previously. Although the individual cross vectors were barely distinguishable above background, the cumulative effect of these very weak interactions made the correct choice unambiguous.

(d) *Absolute protein configuration and phase determination*

Approximate protein phases were calculated from the single uranyl acetate derivative (Blow & Rossmann 1961) without including anomalous scattering. They were used to compute anomalous dispersion difference Fourier maps (Strahs & Kraut, 1968) for the native crystal and for the mersalyl derivative. Large negative peaks were found at the expected iron site and the expected iron and mersalyl sites respectively. This indicated that the original choice of configuration for the iron sites was incorrect. Therefore, the absolute configuration of the protein molecule was established.

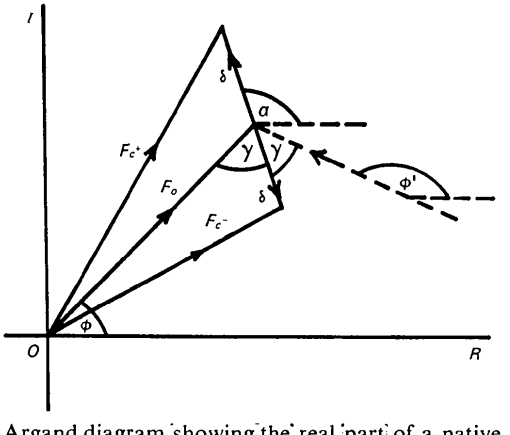

Fig. 1. Argand diagram showing the real part of a native protein structure factor combining with the imaginary contribution of a naturally occuring anomalous scatterer. The mirror image of the vector diagram of the $\bar{h}\bar{k}\bar{l}$ reflection is superposed on the vector diagram of the hkl reflection. The symbols are defined in the text. The two ambiguous phase angles for the native protein are indicated by φ and φ'.

Table 1. *The sum of the derivative anomalous difference Patterson densities at the four cross-vector positions between the iron and heavy atom sites*

'Origin' refers to the fraction of the unit-cell dimension added to the position of the heavy atom. *E* indicates that the hand of the heavy atom sites is inverted. *S*1 and *S*2 are the four vector sums for the atom pairs Fe–U_1 and Fe–U_2, the major uranyl binding sites; *S*3 and *S*4 are the analogous sums for the Fe–Hg_1 and Fe–Hg_2 vectors associated with the two mersalyl sites.

Origin	*S*1	*S*2	*S*1+*S*2	*S*3	*S*4	*S*3+*S*4
(0,0,0)	74	34	108	89	80	169
(0,0,0)*E*	4	11	15	47	19	63
(½,0,0)	2	19	21	45	49	94
(½,0,0)*E*	29	11	40	76	14	90
(0,½,0)	30	28	58	30	22	52
(0,½,0)*E*	37	7	44	19	7	26
(0,0,½)	3	29	32	0	2	2
(0,0,½)*E*	17	10	27	7	25	32
(½,½,0)	25	27	52	20	19	39
(½,½,0)*E*	18	19	37	24	11	35
(½,0,½)	14	12	26	6	5	11
(½,0,½)*E*	5	9	14	1	39	40
(0,½,½)	10	30	40	21	22	43
(0,½,½)*E*	11	7	18	48	48	96
(½,½,½)	9	26	35	49	23	72
(½,½,½)*E*	0	8	8	21	63	84

Phases for the structure factors of the native protein were calculated to 2·8 Å resolution based on combined isomorphous replacement and anomalous scattering measurements for the two derivatives (Matthews, 1966). Phase probability distributions based on anomalous scattering from the iron atom in the native protein alone (Matthews, 1969) were also calculated, as described in the next section, and combined with the heavy-atom phases to calculate the final electron density map.

Use of native anomalous scattering to locate heavy atoms

(a) *Phase calculation from iron atom position*

After the structure of cytochrome b_5 had been successfully completed (Mathews, Levine & Argos, 1972) it was realized that the heavy-atom positions, relative origin and the absolute configuration of the protein could have been determined directly from the native anomalous scattering data. This idea was tested by calculating derivative difference Fourier maps using protein phases based on the iron atom position alone.

Approximate protein phases using the iron atom position alone were calculated by the following two methods: one derived by Matthews (1969) and the other following the method of Kartha (1961). The former allows for the most accurate phase calculation since proper weights based on figures of merit are obtained. The latter method is computationally simpler.

Fig. 1 illustrates the probability method, described by Matthews (1969), explicitly for the case where the protein contains anomalous scatterers. Let F_o be the observed structure-factor amplitude for the native protein which is set equal to $F_o^+ + F_o^-/2$, where F_o^+ and F_o^- are, respectively, the measured Friedel amplitudes $F_o(hkl)$ and $F_o(\bar{h}\bar{k}\bar{l})$. Let φ be the proposed phase angle for $\mathbf{F}_o$. α is the phase angle of $\boldsymbol{\delta}$, the anomalous scattering vector of the iron atom which contributes to the calculated structure factor $\mathbf{F}_c$. Let F_c' be the difference between the calculated Friedel structure amplitudes, $(F_c^+ - F_c^-)$; F_o' is the difference between the observed Friedel structure amplitudes, $(F_o^+ - F_o^-)$.

According to Blow & Crick (1959), the relative probability $P(\varphi)$ of any particular φ being the correct phase for $\mathbf{F}_o$ is given by

$$P(\varphi) = N' \exp\left[-X(\varphi)^2/2E^2\right] \tag{1}$$

where N' is the normalizing factor, E represents the r.m.s. error associated with the measured Friedel pairs, and $X(\varphi)$ is $(F_c' - F_o')$, which is the difference between calculated and observed Friedel differences. It can be easily shown from Fig. 1 that

$$(F_c^+)^2 = F_o^2 + \delta^2 + 2F_o\delta\cos(\alpha - \varphi)\,, \tag{2}$$

and

$$(F_c^-)^2 = F_o^2 + \delta^2 - 2F_o\,\delta\cos(\alpha - \varphi)\,, \tag{3}$$

so that

$$(F_c^+)^2 - (F_c^-)^2 = 4F_o\,\delta\cos(\alpha - \varphi)\,. \tag{4}$$

As δ is normally small compared with F_o (North, 1965),

$$F_o \simeq \frac{F_c^+ + F_c^-}{2}\,, \tag{5}$$

so that

$$F_c^+ - F_c^- = F_c' \simeq 2\delta\cos(\alpha - \varphi)\,. \tag{6}$$

Thus,

$$X(\varphi) = 2\delta\cos(\alpha - \varphi) - (F_o^+ - F_o^-)\,. \tag{7}$$

Using equation (7) in equation (1), a probability distribution can be calculated for various φ and the centroid of the phase probability distribution can be determined, giving the 'best' phase angle and the figure of merit (m) of the phase determination (Matthews, 1969). These approximate protein phase angles and figures of merit, based on the iron anomalous scattering, may then be used to calculate a difference Fourier to determine the location of the heavy atoms in a derivative.

Another formulation, analogous to that of Kartha (1961), is also shown in Fig. 1. The two most probable phase angles for $\mathbf{F}_o$ are φ and φ' which are respectively $(\alpha - \gamma)$ and $(\alpha + \gamma)$ where γ can be calculated from

$$\cos\gamma = [\delta^2 + F_o^2 - (F_c^-)^2]/(2\delta F_o)\,. \tag{8}$$

Let F_H and F_P be the observed structure amplitudes for the derivative and native protein structure respectively. The difference Fourier series to locate heavy atoms using both possible phases (Kartha, 1961) then becomes

$$\begin{aligned}\Delta\varrho(x,y,z) &= \sum_h \sum_k \sum_l (F_H - F_P)\,\{\exp[+i(\alpha+\gamma)] \\ &\quad + \exp[+i(\alpha-\gamma)]\}\exp[-2\pi i(hx+ky-lz)] \\ &= \sum_h \sum_k \sum_l [2\cos\gamma(F_H - F_P)]\exp(i\alpha) \\ &\quad \times \exp[-2\pi i(hz+ky+lz)]\,. \end{aligned} \tag{9}$$

The Kartha method thus essentially chooses the phase angle α of $\boldsymbol{\delta}$ to be the correct protein phase with the weighting factor $2\cos\gamma$. In the probability method, since the distribution function will be symmetrical about $\boldsymbol{\delta}$ [equations (1) and (7)], the centroid of the phase probability distribution will yield $\pm\alpha$ as the 'best' phase angle (North, 1965). The figure of merit will approach unity as the two alternative phase angles in the bimodal distribution coalesce. The two methods thus become equivalent in the choice of protein phase, but differ in the weighting scheme.

(b) Ghost peaks and absolute protein configuration

According to Kartha (1961) the single isomorphous replacement method will yield the correct structure with unit weight plus several ghost images of the inverse structure with lower weight. These ghost images will be located at points corresponding to the Fourier transform of the function $\exp[2i\alpha(hkl)]$ where $\alpha(hkl)$ are the phase angles of the replaceable group. In the present case, where α refers to the phase angle of the anomalous scattering vectors of the iron atoms, the inverse ghost images will be negative and located at the sums of the iron vectors taken pairwise. Thus, with N anomalous scatterers at $\mathbf{r}_i$ there will be (*a*) N inverse negative ghost images with weight $1/N$ centered at positions $2\,\mathbf{r}_i$ and (*b*) $N(N-1)/2$ inverse negative ghost images with weight $2/N$ centered at $\mathbf{r}_i + \mathbf{r}_j$. If $N=4$ there will be 1 full weight true image, 6 half weight negative ghost images and 4 quarter weight negative ghost images, provided the anomalous scatterers are not related by a center of symmetry. In space group $P2_12_12_1$, for example, the 6 half weight ghost images of an atom at X, Y, Z will occur at $(X, Y, \bar{Z} \pm 2Z_{\mathrm{Fe}})$, $(X, \bar{Y} \pm 2Y_{\mathrm{Fe}}, Z)$ and $(\bar{X} \pm 2X_{\mathrm{Fe}}, Y, Z)$.

The nature of the heavy-atom difference Fourier based on native anomalous scattering will depend on the choice of configuration for the anomalous scattering set. $\boldsymbol{\delta}$ may be written

$$\boldsymbol{\delta} = a' + ib'$$

where

$$a' = -\sum_{n=1}^{N} f_n''(\mathbf{h})\sin(2\pi\,\mathbf{h}.\mathbf{r}_n)$$

and

$$b' = \sum_{n=1}^{N} f_n''(\mathbf{h})\cos(2\pi\,\mathbf{h}.\mathbf{r}_n)\,. \tag{10}$$

h represents the reciprocal lattice vector (h,k,l); $\mathbf{r}_n$ is the position vector (x,y,z) of the nth atom in the unit cell; and f_n'' is the imaginary scattering factor component of the nth anomalous scatterer.

Now, if the wrong configuration is chosen for the anomalous scatterer (*i.e.* $\mathbf{r}_n$ becomes $-\mathbf{r}_n$), δ becomes δ_E which is equal to $-a'+ib'$. The phase angle α_E is then $(\pi-\alpha)$. The heavy-atom difference Fourier with phases based on the δ_E calculation will locate heavy atoms at their inverse position with negative electron densities. This is shown by

$$\begin{aligned}\Delta\varrho_E(-\mathbf{r}) &= \sum\sum\sum 2W(F_H-F_p)\cos(-\mathbf{h}\,.\,\mathbf{r}-\alpha_E)\\ &= \sum\sum\sum 2W(F_H-F_p)\cos(-\mathbf{h}\,.\,\mathbf{r}-\pi+\alpha)\\ &= \sum\sum\sum -2W(F_H-F_p)\cos(\mathbf{h}\,.\,\mathbf{r}-\alpha)\\ &= -\Delta\varrho(\mathbf{r}),\end{aligned}$$

where the summation is over a unique hemisphere of reflections and W is m for the probability method and $(2\cos\gamma)$ for the Kartha method. Neither the $\cos\gamma$ factor nor the figure of merit change if the wrong configuration is chosen.

(*c*) *Cytochrome b_5 as an example*

For the probability method the phases were calculated with a refinement program written for the isomorphous replacement method by Dr Hilary Muirhead and modified in this laboratory to include native anomalous scattering data. The error E was taken to be 0·117 of the root mean square lack of closure of the isomorphous phase triangles for the uranyl derivative in the final cycle of refinement at 2·8 Å resolution. This multiplier is the product of two factors, $\frac{3\cdot3}{9\cdot4}\times\frac{1}{3}$. The first is the ratio of the relative mean difference due to anomalous scattering for the native and uranyl data. The second is the factor suggested by North (1965) to apply to the isomorphous r.m.s. error to obtain the anomalous error.

Table 2(*a*) and (*b*) compares the cytochrome b_5 protein phases calculated from the probability method using the iron atom position alone and from the typical heavy atom method as functions of the figure of merit and $(\sin\theta)/\lambda$. The average figures of merit for the isomorphous replacement phases and iron anomalous phases are 0·88 and 0·21 respectively. The average angular difference between the phase angles determined by the two methods is 54° for 1708 non-centric reflections at 2·8 Å resolution. During the phase calculation based on the iron atom alone, the 'occupancy' of the iron was allowed to vary. Since the iron is covalently bound to the protein, the resulting scale factor gives a direct measure of the absolute scale of the protein structure factors. The resulting scale factor of 0·111 agrees favorably with the value of 0·136 obtained from a Wilson (1942) plot of the 2·0 Å native data.

Table 2. *Average protein phase angle differences* (°)

(*a*) For phases determined by the isomorphous replacement method and the probability method using iron anomalous data alone

'FM-Fe' is the figure of merit interval for the iron anomalous case. The table indicates that the figure of merit is a good indication of the correctness of the iron anomalous phases.

FM–Fe	Average protein phase angle difference	Number of reflections
0·00–0·04	76·3	268
0·04–0·08	66·6	243
0·08–0·12	55·4	196
0·12–0·16	58·2	152
0·16–0·20	57·3	114
0·20–0·24	49·5	137
0·24–0·28	41·8	91
0·28–0·32	42·4	87
0·32–0·36	44·7	73
0·36–0·40	43·3	73
0·40–0·44	32·1	40
0·44–0·48	36·2	42
0·48–0·52	30·6	40
0·52–0·56	28·9	35
0·56–0·60	27·1	33
0·60–0·46	21·0	26
0·64–0·68	31·6	20
0·68–0·72	24·7	13
0·72–0·76	24·1	17
0·76–0·80	19·5	8

(*b*) For phases determined by the isomorphous replacement and iron anomalous (probability) methods

'AV FM IR' and 'AV FM Fe' are the average figures of merit for reflections whose phases were calculated from the isomorphous replacement or iron anomalous data respectively for the $\sin\theta/\lambda$ interval concerned.

Average $\sin\theta/\lambda$	AV FM IR	AV FM Fe	Average protein phase angle differences	Number of reflections
0·049	0·948	0·230	68·9	16
0·058	0·927	0·238	46·1	22
0·067	0·944	0·279	49·5	34
0·076	0·851	0·227	49·1	41
0·085	0·907	0·236	47·3	56
0·094	0·903	0·232	57·5	65
0·103	0·894	0·224	55·4	82
0·112	0·901	0·250	49·8	101
0·121	0·879	0·234	54·3	115
0·130	0·891	0·237	52·0	135
0·139	0·888	0·222	53·0	166
0·148	0·883	0·194	57·5	173
0·157	0·864	0·211	52·7	208
0·166	0·826	0·192	54·7	227
0·175	0·831	0·181	54·0	265

Protein phases calculated from the iron anomalous data using the probability and Kartha methods were used to calculate heavy-atom difference Fourier maps. The two major uranyl sites and the two mersalyl sites were clearly indicated by the probability method as the highest electron density peaks on the maps, as shown in Fig. 2(*a*) and (*b*). The Kartha maps (not shown) contained higher background noise but clearly indicated the major binding sites. For the Kartha method, if $\cos\gamma$ was calculated to be greater than 1 or less than -1 the value was set at 1 or -1, respectively.

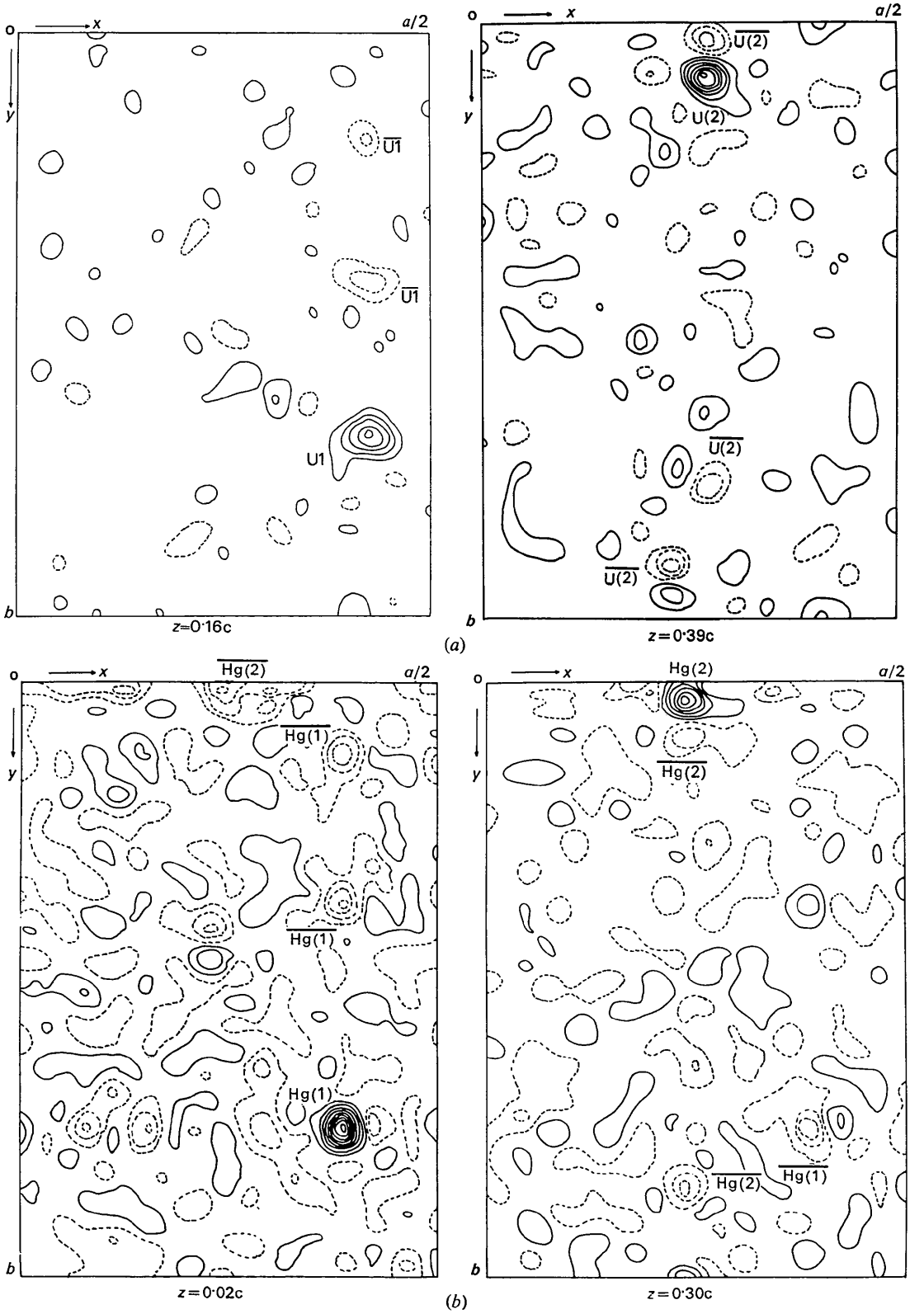

Fig. 2. (*a*) The heavy-atom difference Fourier map for uranyl acetate at 2·8 Å resolution with phases based on the native anomalous scattering data using the probability method. (*b*) as (*a*), for mersalyl. Contours are at arbitrary intervals with the negative contours dashed. The symbols U and Hg refer to the uranyl acetate and mersalyl binding sites, whereas $\overline{\text{U}}$ and $\overline{\text{Hg}}$ refer to the negative ghost images of the uranyl acetate and mersalyl sites, respectively.

It was felt that a weighting scheme based on the magnitude of F_o^+, F_o^- and δ would make the Kartha method nearly equivalent to the probability method.

The negative inverse ghost images, discussed above, were also clearly visible in both difference Fourier maps. Several such ghost peaks are indicated in Fig. 2(*a*) and (*b*). Table 3 lists the peak heights of the true peaks and the six half weight ghost peaks for each of the 6 uranium and 2 mersalyl sites as observed on the respective difference Fourier maps. By correlating each positive peak with its corresponding negative ghost peaks, the 'signal to noise ratio' of the heavy atom sites can be improved.

(*d*) *Cytochrome* b_{562} *as an example*

Presently in this laboratory the structure of cytochrome b_{562} is being studied (Czerwinski *et al.*, 1972).

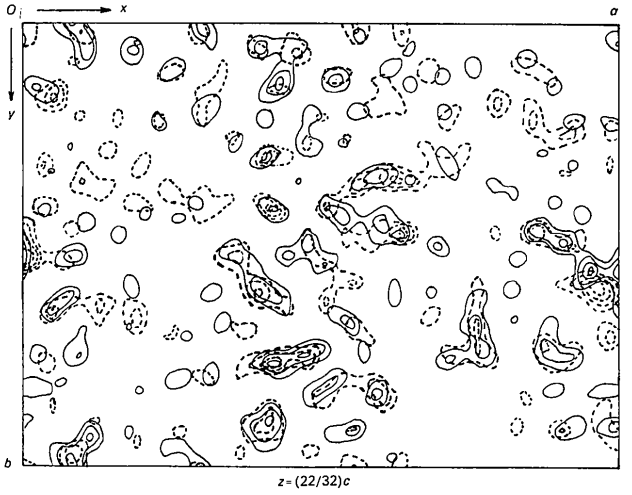

Fig. 3. One section (at $z=22c/32$) of the 3-dimensional electron density map of cytochrome b_5 at 2·8 Å resolution. The solid contours refer to the map based on isomorphous replacement phases and are drawn at intervals of 0·48 eÅ^{-3} starting at 0·58 eÅ^{-3}. The dashed contours refer to the map based on iron anomalous phases and are drawn at intervals of 0·55 eÅ^{-3} starting at 0·71 eÅ^{-3}.

It will provide a further interesting test of the above methods as it is triclinic, $P1$, with 2 molecules per unit cell. It is difficult to locate heavy atoms in this space group. However, if the two iron atoms in the asymmetric unit can be located from the anomalous scattering difference Patterson synthesis, approximate protein phases will be calculated. These phases will be used to try to locate the heavy atom binding sites from the difference Fourier synthesis.

Attempts to determine the protein structure directly from the native data

The protein phases calculated from the anomalous scattering measurements of the native protein crystals were used to compute an electron density map of the native protein at 2·8 Å resolution. The electron density at the iron position was nearly zero owing to systematic coincidence of the positive iron peak and the negative ghost images of the iron atom as described above. The map was much noisier than the one based on isomorphous phases, containing much greater areas of negative density. However, when positive contours were drawn, the anomalous map resembled the isomorphous map surprisingly well, apart from the iron atom effect mentioned above. In particular, the channels of low electron density separating molecules were clearly visible. Fig. 3 shows one section of the map with the isomorphous and the anomalous scattering densities superimposed. The peaks of high density correspond rather well. Fig. 4(*a*) and (*b*) shows stereo views of several sections of the anomalous scattering and isomorphous substitution electron density maps respectively. Also shown are the locations of the α-carbon atoms lying in these sections. As can be seen, the section by section similarity of the two maps is lost when viewed in three dimensions. Attempts to trace the polypeptide chain in the iron anomalous scattering map would undoubtedly lead to severe ambiguities or an incorrect structure. However, certain structural features in three dimensions, such as the helical segment

Table 3. *Peak heights* (e Å^{-3}) *observed on electron density difference Fourier maps of mersalyl and uranyl acetate using phases based on iron anomalous scattering measurements*

For each heavy atom site, the single full weight positive peaks and six half weight negative 'ghost' peaks are listed. The symbols x,y,z refer to the heavy-atom coordinates and $x'y'z'$ refer to twice the iron atom coordinates as described in the text. The occupancy (electrons) and isotropic thermal parameters are taken from Mathews, Levine & Argos (1972). Hg and U refer to the mersalyl and uranyl acetate binding sites respectively.

Atom	Hg(1)	Hg(2)	U(1)*	U(2)	U(3)	U(4)†	U(5)	U(6)†
$\varrho(x,y,z)$	1·02	0·79	1·09	1·52	0·48	0·45	0·70	0·51
$\varrho(x,y,\bar{z}+z')$	−0·49	−0·43	—	−0·90	−0·45	−0·05	−0·49	−0·23
$\varrho(x,y,\bar{z}-z')$	−0·52	−0·37	−0·90	−1·08	−0·47	−0·21	−0·49	−0·22
$\varrho(x,\bar{y}+y',z)$	−0·49	−0.34	−0·53	−0·84	−0·22	−0·24	−0·42	−0·17
$\varrho(x,\bar{y}-y',z)$	−0·44	−0·38	−0·51	−0·65	−0·53	−0·36	−0·30	−0·29
$\varrho(\bar{x}+x',y,z)$	−0·50	−0·35	−0·61	−0·60	−0·24	−0·33	−0·36	−0·12
$\varrho(\bar{x}-x',y,z)$	−0·57	−0·49	−0·55	−0·86	−0·41	−0·13	−0·37	−0·25
Occupancy	42	23	57	50	26	30	32	38
B	22	22	11	7	39	38	41	33

* The positive true peak and first negative ghost peak for U(1) superimpose accidentally.
† The density peaks for U(4) and U(6) are not well defined in the difference Fourier map.

containing residues 84 through 87, are very similar in the two maps.

An attempt was also made to locate the heme group by Patterson superpositions methods. A sharpened Patterson map based on native protein structure factor data to 2·0 Å resolution was calculated. The expected Harker peaks for iron atoms were clearly visible but several other peaks of comparable or higher density were also present. A superposition of the Patterson function on the three iron Harker peaks was carried out using the Buerger minimum function (Buerger, 1959). The minimum function within a 10 Å sphere of the iron atom was plotted on plexiglass sheets but failed to reveal the orientation of the heme group.

Discussion and conclusion

If a protein molecule contains an atom with a significant imaginary scattering factor, *e.g.* iron with 3·4 e a great deal of information can be obtained. The location of the anomalous scatterer can be found from an anomalous scattering difference Patterson map, provided sufficiently accurate X-ray data are available. Experience has shown that diffractometer data, measured by a step-scan procedure and accurate to a few percent, is adequate.

From a knowledge of the iron atom position, the relative origin and configuration of several derivatives can be determined by examining iron–heavy atom cross vectors on anomalous scattering difference Patterson maps. The absolute configuration of the protein can be found from the sign of the iron peak on an anomalous scattering difference Fourier map based on single isomorphous phases. Alternatively, approximate protein phases can be calculated using the iron atom position alone which can (1) show the major binding sites in an unknown derivative by difference Fourier methods, (2) indicate the relative origin and configuration of the binding sites of several derivatives, either known or unknown and (3) reveal the absolute configuration of the protein molecule from the sign of the density of the major peaks in a difference Fourier. Minor binding sites can then be located by the usual cross Fourier or Patterson superposition methods.

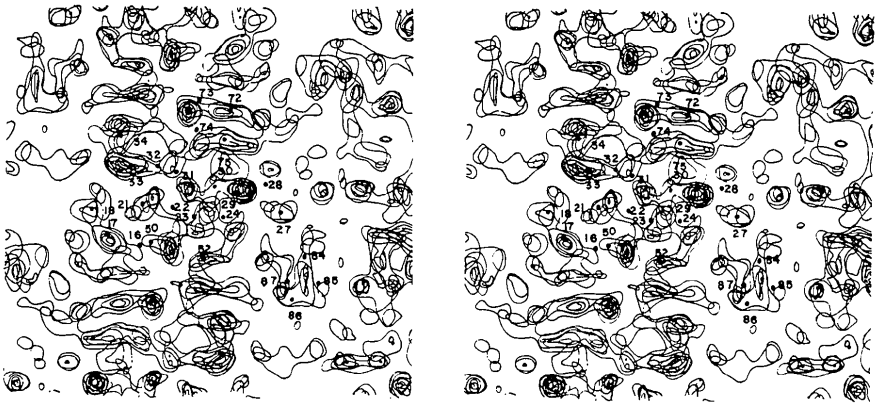

(*a*)

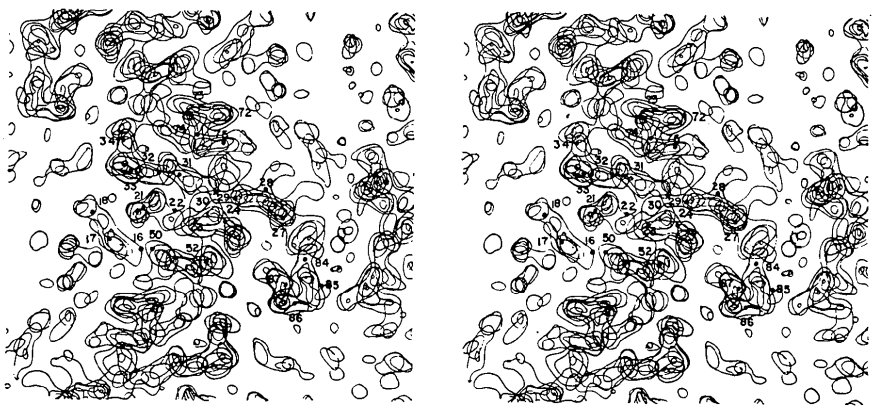

(*b*)

Fig. 4. (*a*) Sections $z=22c/32$ to $z=26c/32$ of the 3-dimensional electron density map of cytochrome b_5 at 2·8 Å resolution based on iron anomalous phases. (*b*) as (*a*) except that isomorphous replacement phases have been used. The contour intervals are as described in Fig. 3. The numerals on each map refer to the α-carbon atoms, indicated by solid circles, which lie within these sections. As can be seen, the continuity of electron density follows the numerical sequence of residues much more closely in (*b*) than in (*a*).

The native anomalous phasing method will have greatest application to cases where poor occupancy or multiple substitution occurs, making direct interpretation of isomorphous difference Pattersons difficult. Alternatively, this method may be useful for locating relative origins for the binding sites from several derivatives in unfavorable space groups, such as $P1$. The major reasons for the success of the method are that full occupancy of the native anomalous scatterer always occurs, the number and types of binding sites are chemically defined, and the X-ray data are inherently more accurate, since no scaling is needed for anomalous pairs and lack of isomorphism never occurs.

The authors wish to thank Drs B. Matthews and G. Kartha for helpful discussions. This work has been supported by NSF Grant No. GB27683 and Life Insurance Medical Research Fund No. G-70-28. P.A. was supported by a U.S.P.H.S. postdoctoral fellowship.

References

BLOW, D. M. & CRICK, F. H. C. (1959). *Acta Cryst.* **12**, 794–802.

BLOW, D. M. & ROSSMANN, M. G. (1961). *Acta Cryst.* **14**, 1195–1202.

BUERGER, M. J. (1959). *Vector Space*. New York: John Wiley.

CZERWINSKI, E. W., MATHEWS, F. S., HOLLENBERG, P., DRICKAMER, K. & HAGER, L. P. (1972). *J. Mol. Biol.* **71**, 819–821.

International Tables for X-ray Crystallography (1962). Vol. III p. 213. Birmingham: Kynoch Press.

KARTHA, G. (1961). *Acta Cryst.* **14**, 680–686.

KRAUT, J., STRAHS, G. & FREER, S. T. (1968). In *Structural Chemistry and Molecular Biology*, edited by A. RICH & N. DAVIDSON, p. 55. San Francisco: Freeman.

MATHEWS, F. S., LEVINE, M. & ARGOS, P. (1972). *J. Mol. Biol.* **64**, 449–464.

MATTHEWS, B. W. (1966). *Acta Cryst.* **20**, 82–86.

MATTHEWS, B. W. (1969). In *Crystallographic Computing*, edited by F. R. AHMED, p. 146. Copenhagen: Munksgaard.

NORTH, A. C. T. (1965). *Acta Cryst.* **18**, 212–216.

STRAHS, G. & KRAUT, J. (1968). *J. Mol. Biol.* **35**, 503–512.

WILSON, A. J. C. (1942). *Nature, Lond.* **150**, 152.

WYCKOFF, H. W., DOSCHER, M., TSERNOGLOW, D., INAGAMI, T., JOHNSON, L. N., HARDMAN, K. D., ALLEWELL, N. M., KELLY, D. M., & RICHARDS, F. M. (1967). *J. Mol. Biol.* **27**, 563–578.

Acta Cryst. (1973). B**29**, 1611

Peri Interactions: An X-ray Crystallographic Study of the Structure of 1,8-Bis(dimethylamino)naphthalene*

BY HOWARD EINSPAHR,† J.-B. ROBERT,‡ RICHARD E. MARSH AND JOHN D. ROBERTS

Gates, Crellin, and Noyes Laboratories of Chemistry, California Institute of Technology, Pasadena, California 91109, *U.S.A.*

(*Received* 11 *December* 1972; *accepted* 21 *February* 1973)

Crystals of 1,8-bis(dimethylamino)naphthalene, $C_{14}H_{18}N_2$, are orthorhombic, space group $P2_12_12_1$, with $a=12{\cdot}855$ (1), $b=10{\cdot}110$ (1), $c=9{\cdot}664$ (1) Å and $Z=4$. A complete structure determination, including refinement of the positions of the hydrogen atoms, led to an R index of 0·053 and a goodness-of-fit of 2·02 for 1477 reflections. The molecule adopts a conformation in which one carbon atom of each of the dimethylamino groups is eclipsed with respect to the naphthalene ring. Hindrance between the dimethylamino groups and/or resonance interactions between the dimethylamino groups and the aromatic ring are sufficiently great to distort the ring in several ways, the most conspicuous being a sizable increase in the non-bonded C(1)···C(8) distance (2·56 Å) compared to the C(4)···C(5) distance (2·44 Å) and a twisting of the naphthalene ring into a considerably nonplanar conformation.

Introduction

The title compound, *N,N,N′,N′*-tetramethyl-1,8-diaminonaphthalene (I), is especially interesting for its unusual basic properties ('the proton sponge'; Alder, Bowman, Steele & Winterman, 1968) and for the steric effects which are expected to be encountered and their influence on the conformation that the molecule will find most favorable. Normally, there is strong resonance interaction between a dimethylamino group and an aromatic ring, so that one might expect a planar conformation to be favored (*cf.*, *e.g.* Wheland, 1955). However, because of the steric difficulties for compounds such as (I), there is no reasonable possibility of bringing even one of the dimethylamino groups into the plane of the ring. Alternative possibilities include (II), where

* Contribution No. 4507 from the Division of Chemistry and Chemical Engineering, California Institute of Technology. This work was supported in part by a grant from the National Science Foundation, and in part by grant GM 16966 from the Division of General Medical Sciences, Public Health Services.

† Present address: Institute for Dental Research, University of Alabama Medical School, Birmingham, Alabama, U.S.A.

‡ Present address: Centre d'Etudes Nucléaires de Grenoble, 38-Grenoble, France.